Astron. Astrophys. 325, 915–922 (1997)

ASTRONOMY
AND
ASTROPHYSICS

Surface photometry of the edge-on spiral NGC 4565⋆

I. V-band data and the extended optical warp

Magnus Näslund and Steven Jörsäter

Stockholm Observatory, S-133 36 Saltsjöbaden, Sweden (magnus@astro.su.se, steven@astro.su.se)

Received 5 July 1996 / Accepted 13 January 1997

Abstract. We have studied the faint luminous parts of the disk of NGC 4565 in the radial and z-directions. The semi-major axis profiles follow exponentials until a break in the luminosity profiles occurs. Beyond the breaks the luminosity distributions are well fitted by steeper exponentials and continue with a constant slope to the limit of the data around $\mu_V = 28$ mag/□″.

A recent discovery of a faint luminous halo in NGC 5907 has raised the question whether there is a luminous population tracing the dark mass in spiral galaxies. The vertical profiles of NGC 4565 fall off less steeply than those of NGC 5907 which to a large extent is explained by the combination of a thin disk and a photometric thick disk. The outer profiles are more shallow, in agreement with previous studies, giving a hint of a third component or of the response of the inner parts to the dark-halo mass. The constancy of scaleheight with radius in the outer parts is confirmed.

The marginal NW stellar warp is also confirmed, but more interestingly there is a faint extension of this optical warp, which coincides with the H I warp, and therefore most likely is physically connected to the galaxy. This finding indicates that star formation may occur outside the disk cutoff in spiral galaxies.

Key words: galaxies: halos – galaxies: NGC 4565 – galaxies: photometry – galaxies: spiral – galaxies: structure – dark matter

1. Introduction

The 'missing mass', or maybe more appropriate 'missing light', in spiral galaxies is in general ascribed to a dark halo (see e.g. Broeils 1992). Many attempts have been made to challenge this. Valentijn (1990) suggested that spirals might be opaque and hence that more matter is actually present in a disk-like shape than directly observed. Molecular clouds have been proposed as a possible source (Valentijn 1991; Lequeux et al. 1993; Pfenniger et al. 1994).

There have been some attempts over the years to detect an optical counterpart to the dark halo. The search for optical halos has in general been without success (see e.g. Hegyi & Gerber 1977; Kormendy & Bruzual 1978). An interesting exception is the study by Sackett et al. (1994), who claimed to have found a faint luminous halo around the edge-on disk galaxy NGC 5907. This finding has recently been confirmed by Lequeux et al. (1996).

The rarity of investigations of this kind can at least in part be explained by the difficulties of reliably reaching faint levels with photographic methods and the problems of obtaining a wide field-of-view and accurate flatfielding by use of CCDs. We have tried to overcome the problem involved in using a CCD for extended faint galaxy photometry by a) using a focal reducer to get a larger field and combining adjacent fields by mosaicing and b) doing flatfields on the night sky itself to avoid the colour temperature difference introduced by using dome or twilight flatfields, since the night sky dominates the surface brightness completely at the surface brightness levels we are aiming at.

In this paper we present the first results in the V band for the edge-on spiral NGC 4565, as part of a deep surface photometry project that was started to address the following questions:

- Is there a faint optical tracer of the invisible matter responsible for the flat rotation curves?
- Are there radial and/or vertical colour gradients revealing the presence of dust or changes in populations?
- What is the extent of optical warps?

NGC 4565 has previously been studied photometrically (e.g. Hamabe et al. 1980; Jensen & Thuan 1982; Van der Kruit 1979; Van der Kruit & Searle 1981a) as well as in H I (Sancisi 1976; Rupen 1991). Shaw & Gilmore (1989) used the data of Jensen & Thuan to model the luminosity distribution, while Florido et al. (1991) focused on the optical warp of this and two other edge-on galaxies.

We briefly describe the observations and reductions in Sects. 2 and 3, respectively. In Sect. 4 we present the results

Send offprint requests to: M. Näslund

⋆ Based on observations collected at the Nordic Optical Telescope, La Palma, Spain

and a summary is given in Sect. 5. We will use the same distance to NGC 4565 (10 Mpc) as most of the references above.

2. Observations

The present observational material was obtained in two runs with the 2.56 m Nordic Optical Telescope (NOT) on La Palma. At the time of the first run (February 14/15 and 19/20, 1991) a Tektronix 512 × 512 CCD camera, called the Stockholm CCD, was the only available detector and we used it together with the Stockholm Focal Reducer (SFR, Jörsäter 1991), resulting in a 5′.4 field with 0″.63/pixel. The data obtained with this equipment constitute our reference material, but will not be discussed in any detail in this paper.

During the second run (February 10/11 1994) we used the IAC Thomson 1024×1024 CCD together with the SFR, yielding a 7′ effective field and 0″.462/pixel, and with this instrumental setup we re-mapped NGC 4565 in the V band. The apparent size of the galaxy (16′) made it extend far outside a single frame and mosaicing became necessary. We collected 11 images in total and the exposure time per pixel in the combined image is about 25 minutes.

The sky background level is easily obtained with the focal reducer, and a decent resolution is preserved which is necessary in order to subtract stars and background galaxies, but focal reducers also have problems. Internal reflections, giving rise to a phenomenon called sky concentration, is the most serious one. This problem is especially bad in optical systems which have parallel beams suited for grism spectrography. The SFR avoids parallel beam sections and the sky concentration phenomenon is kept low.

In connection with the galaxy mapping procedure the telescope was moved about 30′ in different directions from the object, in order to obtain 'blank-sky' frames. These are believed to be sufficiently far away from the object to be free from galaxy light, but close enough to map the 'same' sky. The total exposure time of the flatfields is 50 minutes. Images of the twilight sky and dome flats were also obtained for reference.

3. Reductions

We describe the most important steps of the reduction procedures briefly below. We have primarily used MIDAS, supplemented in a few cases by IRAF. More details of the reduction procedures can be found in Näslund (1995).

3.1. Flat fields

Flatfielding is a key point when doing deep surface photometry with CCD arrays, and we used frames of the blank sky to get the most accurate large-scale structure of these flatfields. We found that the blank-sky frames had the same large-scale structure and after star-subtraction by use of DAOPHOT the frames were averaged to a master flatfield. By flatfielding the blank-sky frames and measuring the spread of mean intensity over the field of each frame, we estimated the large-scale flatfield residuals to be $1.5 \times 10^{-3}(1\sigma$ rms) of the sky background.

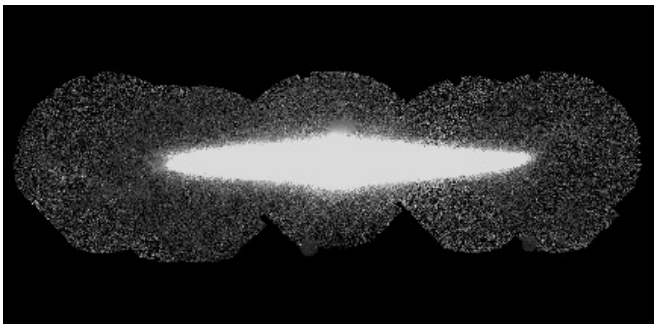

Fig. 1. The combined and rotated image of NGC 4565. The image is a combination of 11 frames and covers an area of approximately $24' \times 7'$. SE is to the left and NW to the right.

3.2. Combination of frames

We used DAOPHOT to remove foreground stars and masked residuals and background galaxies manually. Then the flatfielded, star-subtracted and sky-subtracted object frames were corrected for extinction, using the value found by the Carlsberg Meridian Circle at La Palma on the night in question, followed by a scaling to an exposure time of one second. Then we translated the frames to a common coordinate system, and combined them using the program COMB-CCD in MIDAS to form an almost complete map of the galaxy. In the combination process a careful noise analysis is done pixel by pixel. The method of combination is similar to that of Shaw & Gilmore (1990).

The frames were combined from SE (left in Fig. 1) to NW along the major axis of the galaxy. The overlap between the central frames and the first northwest frame (the first frame to the right of the central frames) is however small, which made the statistics rather poor. As a consequence it was difficult for the program to calculate the correct residual sky in the frames to the right of the centre. By measuring the residual sky at different positions in the combined image we discovered that there was a sudden decrease in sky intensity northwest of the centre, so that all sky positions of the NW part yielded systematically lower values well below any expected noise or flatfield gradients. Because this obviously is an artifact of the combination procedure we combined the frames once more and added the same constant value to the computed residual sky of the northwest frames. This will not affect the analysis below since it has only prevented us from detecting a systematic difference between the NW and SE parts. We find it unlikely that the NW half of the galaxy (as well as the residual sky!) would be systematically fainter than the SE part by a constant value and previous studies of NGC 4565 have not pointed to such an asymmetry.

3.3. Calibration

We used the existing photometry of NGC 4565 to calibrate our combined 'raw' image (neither star subtracted nor smoothed). Jensen & Thuan (1982, henceforth JT) have published V-band aperture photometry for the central region of NGC 4565, obtained by themselves and others. We used the mean of all these values to get the calibration factor needed.

We checked the calibration using standard star observations, and we obtained a calibration factor that yielded a difference of less than 0.08 magnitudes compared with the one determined from the aperture photometry.

4. Results and discussion

Our combined V-band image of NGC 4565 is found in Fig. 1. Several of the published optical investigations concern the central region, but here we will focus on the disk and the corona/halo.

4.1. Radial light profiles

In order to estimate the accuracy of the rotation angle (i.e. the position angle of the major axis) we binned and smoothed the rotated image slightly and extracted an isophote of intermediate brightness well outside the dust lane. Then we determined the midpoint between the upper and lower isophote along a few columns. A line through these midpoints turned out to be horizontal and we therefore conclude that the position angle is fairly accurate.

We first extracted the major-axis profile in the same way as JT for comparison reasons. Because their radial V-band profile was normalized to the corresponding B-band profile we had to shift their V profile by a constant value. The two profiles agree well over most of the range after the shift was applied. The discrepancy is less than 0.1 magnitudes/$\Box''$, except for a few points at the outer parts where the averaged profiles are very sensitive to the position angle chosen, the influence of stars etc.

Before the extraction of the major-axis profile we smoothed the image by a Gaussian of FWHM = 10 pixels. In Fig. 2 we show the profiles of each side of the galaxy centre, obtained by extracting two lines along the major axis. The region around the major axis is however severely affected by dust, and a scalelength R_d more representative of the stellar population is obtained out of the plane. The modelling procedure (Sect. 4.4.2) yields R_d = 5.6 kpc, in accordance with Van der Kruit & Searle 1981a (henceforth KS81a).

The breaks in the exponential profiles are located at radii of 17 kpc (SE) and 20 kpc (NW), which correspond to about 3.0 R_d and 3.6 R_d. The disk cutoff, as defined by KS81a, occurs at 4.5 R_d. Disk cutoffs have earlier been investigated by KS81a and Van der Kruit (e.g. 1988), who found that they generally occur at $4R_d - 5R_d$ (e.g. for NGC 4565), while Barteldrees & Dettmar (1994) arrived at the lower value of $(3 \pm 1)R_d$ for a different sample.

In our data exponentials also provide a good solution at both ends beyond the profile breaks and there is no clear hint in these data of any further change in disk scalelength at surface magnitudes brighter than μ_v = 28 mag/$\Box''$.

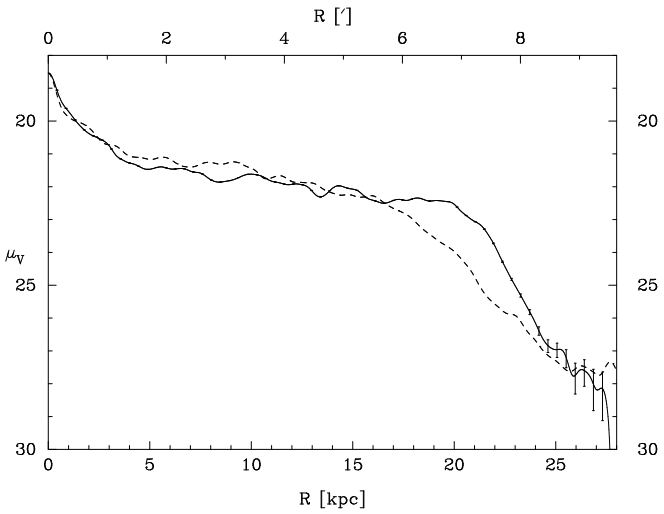

Fig. 2. The semimajor axis profiles of NGC 4565 in the V band. Both profiles are extracted from the rotated and smoothed image. The solid line is the NW profile, the dotted line is the SE profile. A determination of scalelengths from this figure are affected by the presence of dust and possible colour gradients (JT). The error bars represent the combination of Poisson noise, reduced due to the smoothing, and the background fluctuations. The errors are plotted at equally spaced points along the NW profile only.

4.2. Error sources

An error in determining the sky background is perhaps the first error source that comes to mind. The program COMB-CCD (Sect. 3.2) uses the sky from a frame far from the galaxy centre and then compares the overlap between each pair of frames as they are combined, so that the residual sky background of every single frame can be adjusted prior to the combination. This procedure assumes that possible gradients in the sky background have been removed.

Another important effect when dealing with faint emission is instrumental scattered light (Capaccioli & de Vaucouleurs 1983; Morrison et al. 1994; Lequeux et al. 1996). In our case the focal reducer plays a central role. By tracing the light along a line in two individual frames that overlap, we can by comparing these profiles detect scattered light, since it will behave differently in the two frames due to their different offsets relative to the galaxy nucleus. We see no difference larger than the expected errors of the extinction correction. Furthermore, the PSF obtained by averaging the light around stars in concentric circles shows no sign of an extended shallow profile and the faint outer parts of the z profiles of the galaxy are symmetrical (see discussion on z profiles in Sect. 4.4 below), which probably would not have been the case if scattered light made a significant contribution in these areas, unless scattered light behaves identically as the galaxy closer to the minor axis.

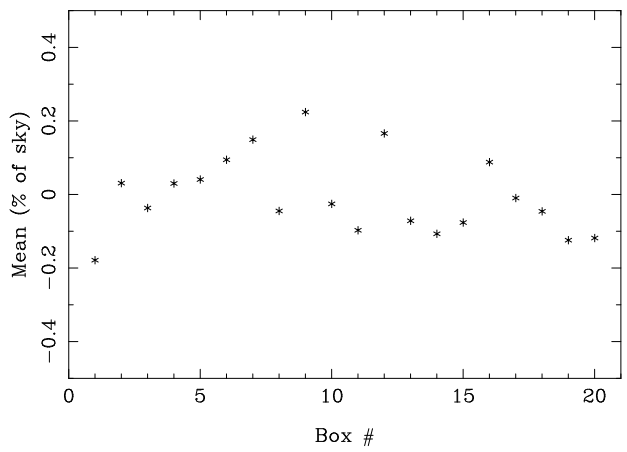

Fig. 3. Mean values of sky regions of size 61 × 61 pixels. Box #1-#12 are at the SE side of the galaxy, while box #13-#20 are located on the NW side. There may be a small residual left between the two sides.

We estimated the precision of our photometry at low levels by calculating the statistics in selected sky areas and we should in this way be able to estimate the systematic effects that are expected at low intensity levels. Fig. 3 shows the spread in the sky background measured in this way. Each point represents the mean value in a square of size 61 × 61 pixels at arbitrary positions free from stars. Boxes 1-12 are chosen east of the SE part of the galaxy, while boxes 13-20 are from the region west of the NW side. The absolute spread is approximately 0.3 % of the mean sky background in the scaled images. At $\mu_{\rm v}$ = 28 the standard deviation of these mean values corresponds to an rms error of -0.3/+0.5 in magnitude.

The scale of 0.″46/pixel is good enough to get a rather deep limit of unresolved background objects, although the resolution is determined by the seeing of about 1″. The presence of background objects will of course show up as fluctuations in the background at some level. However, if these fluctuations increased the sky background value significantly and thereby made us overestimate the sky background, then we expect a turnoff in the exponential decline beyond the physical disk cutoff seen in the major-axis profile. No such effect is seen above $\mu_{\rm v} \approx 28$ mag/□″ in the major axis profile (Fig. 2). Assuming that the beginning of the profile decline is correct we must have a conspiracy by scattered light and an overestimated sky background in order for the luminosity to decline with constant slope.

4.3. Asymmetries

Many disk galaxies are known to have deviations from the flat circular shape, not only in the form of warps, but also as lopsided asymmetries. Most of these asymmetries are found in the gas distribution (Baldwin et al. 1980; Richter & Sancisi 1994), but optical and infrared cases have also been discovered (e.g. Block et al. 1994; Rix & Zaritsky 1995). As an example, M101 is a face-on spiral whose arm structure is clearly asymmetric and by viewing such a galaxy edge-on from the right position angle it may display a lopsidedness like the one seen in Fig. 1 and Fig. 2 for NGC 4565.

In addition, the inner parts of the vertical profiles of NGC 4565 also differ from each other, as will be seen in Sect. 4.4.2.

4.4. Vertical (z) light profiles

KS81a and Van der Kruit & Searle (1981b) investigated several edge-on spirals to determine the radial as well as the vertical light distributions. They showed that the light profiles perpendicular to the plane of their galaxies were well fitted by the isothermal sheet approximation, with a superposed exponential decline in the radial direction:

$$L(R,z) \propto \mathrm{sech}^2(z/z_d) \times e^{-\frac{R}{R_d}}, \quad (1)$$

where R_d and z_d are the disk scalelength and scaleheight, respectively. We have used Eq. (1) as the basic function describing the luminosity distribution of the disk, although other functions have in some cases been found to fit the regions closest to the galactic planes better (e.g. De Grijs & Van der Kruit 1996).

4.4.1. Thick disks

In NGC 4565, the steep decline of the z profiles merges into a shallower profile that can be a sign of a so called thick disk. This type of 'photometric thick disk' have been found in a few edge-on spirals (KS81a; JT; Van Dokkum et al. 1994), while others like NGC 4244 and NGC 5907 seem to lack this kind of excess light (KS81a). The non-detection of a thick disk in NGC 5907 has been confirmed with deeper data by Morrison et al. (1994).

It is still an open question if this excess light at intermediate levels is a discrete component, but various detailed studies of star samples (e.g. Carney et al. 1989; Edvardsson et al. 1993; Robin et al. 1996) give evidence for a discrete thick-disk component in the Milky Way Galaxy.

A somewhat different explanation was given in a recent letter by Fuchs (1995) who interpreted the shallow faint halo of NGC 5907 as the result of the interaction between the dark halo and a 'normal' stellar halo with a density profile declining as $r^{-3.5}$. On the same basis he explained the outer z^{-2} profile of NGC 4565 as the response of the inner bulge to the dark mass distribution.

4.4.2. Our profiles

We masked the dust lane along the major axis and binned the unmasked parts with bin sizes increasing exponentially both in the R and z directions. As a result of the masking the data with $z \lesssim 1$ kpc were excluded. The radial extent of the input to the modelling was restricted to $2' \leq R \leq 5'$ to isolate the disk from bulge light and warp effects. Even though the asymmetries that were pointed out above suggest that the NW and SE parts of the galaxy should be modelled separately, the gaps of spatial coverage prohibit stable solutions in a few cases, so we decided to use all the available data together.

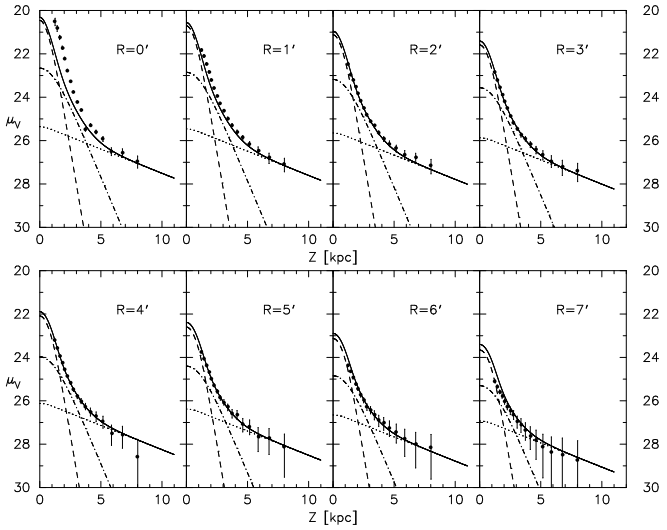

Fig. 4. Vertical profiles at positions separated by $1'$ in the radial direction. Each point is the average of the values at the four (two in the case of the minor axis) symmetrical positions around the centre. The error bars represent typical variations at the corresponding surface-brightness level. In a few cases less than four sectors have been used due to lack of data at some positions or image defects. The lines are the result of the three-disk fit, with the solid lines displaying the sum of the individual components. However, only regions in the range $2' \leq R \leq 5'$ were used in the fit.

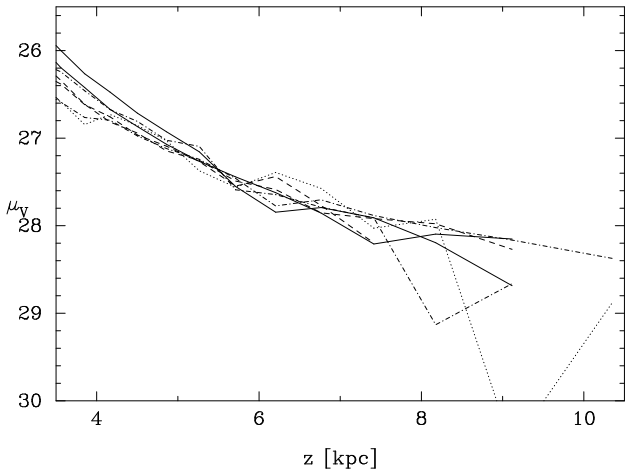

Fig. 5. Vertical profiles shifted to overlap with the $R = 5'$ profile for $z \geq 4$ kpc. The two deviating points at $z > 8$ kpc were excluded from the calculation of the shift of this profile.

Fig. 4 shows the vertical profiles extracted at every integer arcminute along the major axis of the rotated and masked image. The points represent the mean value in bins 100 pixels wide and with a height exponentially increasing from the major axis. The points are also averages of points at symmetrical positions around the centre, i.e. most points in the figure are the mean of four (except the minor axis), but in a few cases less than four points were used due to gaps in spatial coverage or image defects. Even though NGC 4565 has asymmetries like the warp and the lopsidedness it seems to be symmetric on large scales outside the central plane.

In Fig. 5 we have shifted the profiles vertically so as to make them overlap with the $R = 5'$ profile for $z \geq 4.0$ kpc. The profiles agree very well, which shows that the faint parts at high galactic latitude of the galaxy display a high degree of symmetry and confirm the constancy of scaleheight with R at these z.

Previous investigations (JT; Shaw & Gilmore 1989, henceforth SG89) point to a rather complex structure consisting of three components, the bulge excluded, and for this reason we used a few different functions to fit the binned two-dimensional map of the galaxy. Because the modelling procedure yields rather large reduced chi-square (χ^2_ν) values of the order of 6, we are probably left with some systematics or an insufficient model. However, it turns out that almost every bin with a substantial residual compared with the model is located close to the dust mask along the major axis and might hence be affected by unmasked dust features or other asymmetries in the light distribution. The faint parts of the galaxy that are of most concern to us here are however well fitted by the modelling procedure.

We have used a few different combinations of galaxy components where Eq. (1) is the basic one, here called the one-disk model. The two-disk model is a sum of two sech^2 functions like Eq. (1), while the three-disk model is a three-component model similar to the type used by SG89, with the third component looking like

$$L(R,z) \propto e^{-|\frac{z}{z_e}|}\, e^{-\frac{R}{R_d}}. \tag{2}$$

We have also used the one-disk and two-disk models together with a powerlaw halo, modelled as

$$\frac{\rho_0}{\left[1+\frac{R^2+(\frac{z}{q})^2}{R_0^2}\right]^{(\gamma/2)}}, \tag{3}$$

where q is the halo flattening and R_0 is the core radius. In addition, we substituted the sech^2 functions with exponentials, but with only minor differences as a result. Some of the parameters, like the halo flattening and γ, were often held fixed to constrain the modelling somewhat. The results are summarized in Table 1 where the reduced chi-square $\chi^2_{\nu,\mathrm{rel}}$ is measured relative to the χ^2_ν of the three-disk model. The three-disk model is shown in Fig. 4 and the 'best-fit' parameters are found in Table 2. It is clear from Table 1 that we have not been able to separate one 'outstanding' model from the others, either because of the complex light distribution or that we are not using the right functions. There is also a problem of finding the absolute minimum in parameter space when many parameters are involved, but we tried to minimize this problem by varying the initial guesses around values found by others, for this and other galaxies, or by keeping some of the parameters fixed. A graphical example of a few of the different models is given in Fig. 6.

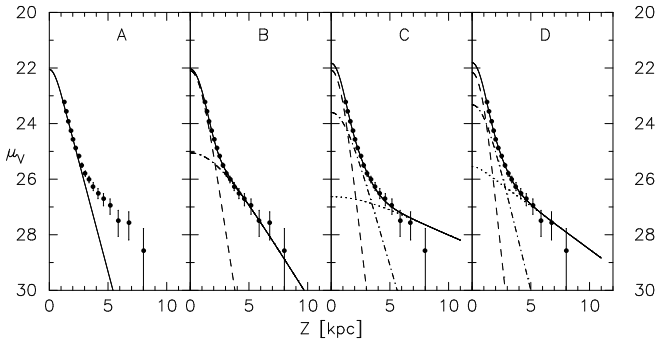

Fig. 6. Comparison of different models at $R = 4'$. The models are (from left to right): Single exponential, two-disk model, two-disk + halo ($\gamma = 3.5, q = 0.5$) model and three-disk model.

Table 1. Modelling results. Note that $\chi^2_{\nu,\mathrm{rel}}$ is a number *relative* to the χ^2_ν of the three-disk model. The three-disk model yields $\chi^2_\nu = 6$ for 1963 degrees of freedom (see text for discussion). The first result for the three-disk model in the table was obtained with the central luminosity density of the second disk component held fixed at a value of 5% of the first component. Parameters that were held fixed are marked with (f). The last column contains references to the models displayed in Fig. 6.

Model	$\chi^2_{\nu,\mathrm{rel}}$	Note	Ref.
One-disk	2.93		A
One-disk + halo	1.29	$q = 1$ (f), $\gamma = 2.0$ (f)	
	1.28	$q = 1$ (f), $\gamma = 3.1$	
	1.19	$q = 0.5$ (f), $\gamma = 2.0$ (f)	
	1.12	$q = 0.5$ (f), $\gamma = 3.5$ (f)	
Two-disk	1.09		B
Two-disk + halo	1.02	$q = 1$ (f), $\gamma = 2.0$ (f)	
	1.02	$q = 1$ (f), $\gamma = 3.5$ (f)	
	1.01	$q = 0.5$ (f), $\gamma = 2.0$ (f)	
	1.01	$q = 0.5$ (f), $\gamma = 3.5$ (f)	C
Three-disk	1.01	$L_{0,\mathrm{thick}} \approx 5\%$ of $L_{0,\mathrm{thin}}$ (f)	
	1.00		D

If the division of the luminosity profiles into exponential or exponential-like functions is appropriate, which may be justified by the investigations of the Milky Way Galaxy (e.g. Robin et al. 1996), then a one-disk model provides such a bad fit that a second component, either a thick disk or a faint luminous halo must be introduced. Even a two-component model seems to leave residual light at high z, indicating the presence of a third component or that the other two functions do not provide the right solution. As noted above, a three-component model as the one used by SG89 or a 'two-disk + halo' model provide in principle equally good fits to our data. There is thus no clear evidence of a density component dropping as r^{-2} above $\mu_V = 28$ in NGC 4565 as found by Sackett et al. (1994) for NGC 5907.

If there is an optical r^{-2} halo in this galaxy it is hidden among the other components or it is fainter than our photometric limit. It is still possible that deeper data may reveal a more

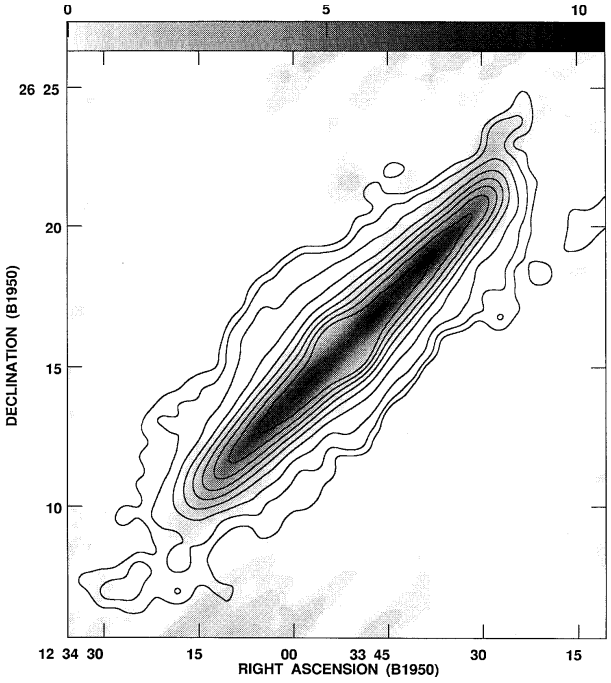

Fig. 7. The smoothed combined image of NGC 4565 as contours and the H I data of Rupen (1991) as grey scale.

Table 2. Best-fit parameters of the three-disk model. Note that the central surface brightnesses are not well constrained due to the lack of data caused by dust masking.

Parameter	Comp. 1	Comp. 2	Comp. 3
$\mu(0,0)$[mag/$\Box''$]	20.2	21.8	24.6
R_d [kpc]	5.6	5.9	9.6
z_d; z_e [kpc]	0.6	1.3	3.5

distinct halo-like component. In addition, a more uniform coverage would permit a more detailed modelling in the sense that different parts of the galaxy could be modelled separately to account for the asymmetries mentioned earlier.

Furthermore, a large deep sample of well studied galaxies of different morphological types, bulge strengths etc., preferably combined with stellar kinematics (Shaw 1995), are probably needed to settle the question of the presence of thick disks in spirals and S0 galaxies.

4.5. The warp

NGC 4565 exhibits a warp at either end of the disk. The NW warp is clearly seen in H I (Sancisi 1976), but is less prominent in optical bands (Van der Kruit 1979). The SE side is less strongly warped in H I and marginally detected optically, and is in addition difficult to trace down to faint levels due to the crowding of background objects in this region. However, on the NW side our V-band data reveal a faint structure at a level

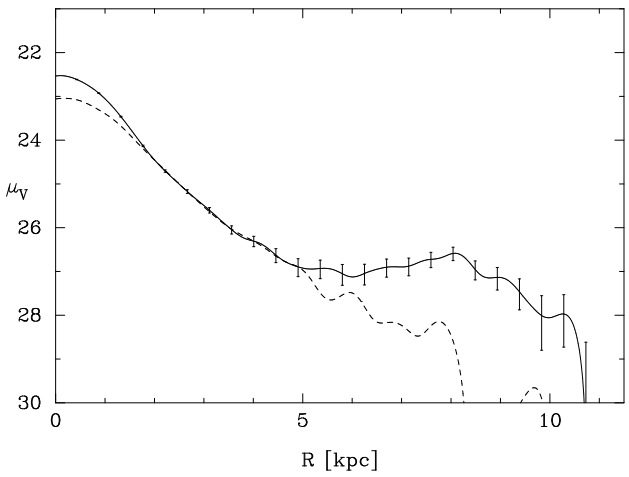

Fig. 8. A cut starting in the galaxy plane, 20 kpc from the centre, through the maximum intensity of the warp, at an angle of 32.°9 relative to the major axis (solid line). The dashed line shows a cut parallel to the one through the warp, but starting closer to the centre. This curve has been shifted so that the exponential parts of the two profiles overlap between 2 and 4 kpc. The error bars are as in Fig. 2.

of $\mu_V \approx 27$ mag/$\Box''$ beyond the 'optical' disk, reported by Näslund (1995) and Näslund & Jörsäter (1995). In Fig. 7 the V-band image is represented by contours, while the H I observations by Rupen (1991) are in grey scale. The faint feature is seen to align well with the H I warp and if it is physically connected to the galaxy it is to our knowledge the first detection of an optical counterpart to an extended 'radio' warp. A trace across the maximum intensity of the optical warp is shown in Fig. 8, and Fig. 9 displays a contour plot of the feature.

We have detected the feature at the same celestial position in different images, and in images obtained without the focal reducer and with yet another CCD. This fact excludes the possibilities that the warp feature is an effect of flatfield irregularities or a ghost image. We can however not rule out the possibility of this feature being an unresolved distant galaxy cluster (see Dalcanton 1996).

The fact that the feature is overlapping the H I warp makes us believe that we have found optical emission outside the continuous disk, at a distance of approximately 27 kpc from the centre of the galaxy. This is certainly a large distance, but corresponds roughly to the distance of the H II region in the Milky Way Galaxy discovered by De Geus et al. (1993), which indicates that luminous regions may be found this far from the galaxy centre. The total luminosity of this region is approximately $5 \times 10^5 L_{V_\odot}$. Rupen (1991) calculated the total H I content of the NW warp to be $7 \times 10^8 M_\odot$ and we estimated from his data that the outer parts corresponding to the optical outer warp, contain about $1.5 \times 10^8 M_\odot$ of H I. The ratio of H I mass in solar units to $L_{V_\odot}$ is thus ~ 300.

In order to obtain more information on the nature of this feature we will study the galaxy at different wavelengths, which will be discussed in a forthcoming paper. *If* the extended warp consists of an older population like K or M stars (B-V $\approx$ 1, V-R $\approx$ 1) it would be possible to detect it in the B band as well as in the R band, considering the typical nightsky brightness in these wavelength bands. A young population or light scattered by dust is on the same grounds expected to be clearly visible in the B band. It is at this stage difficult to draw any conclusions on the origin or source of the warp, but its coincidence with the gaseous H I warp at these large radii, does not point to a separation of the stellar and the gaseous warps as claimed by Florido et al. (1991). Consequently this finding seems to be in contradiction to the proposal of warps being the result of magnetic field interaction. A superposition of optical and H I warps have also been found in NGC 7814 by Lequeux et al. (1995) and in UGC 7170 by Cox et al. (1996).

5. Summary

We have been studying the following properties of NGC 4565 in the V band:

- The major axis profile
- Profiles perpendicular to the disk
- The NW warp

The major axis profile of NGC 4565 exhibits the characteristic exponential decline followed by a sharp break beyond which the luminosity follows a steeper exponential. The galaxy is asymmetric in the sense that the NW side has a shallower profile and a steeper cutoff compared with the SE side. By tracing the profiles at a constant position angle we could not find any signs of changing scalelengths above μ_V = 28 mag/$\Box''$ beyond the breaks.

The most remarkable finding in this data is revealed if we follow the bending of the stellar warp on the NW side. A faint feature ($\mu_V \approx 27$ mag/$\Box''$) is seen already in the 'raw' image, but is more clearly displayed in a smoothed version of the combined image. This structure aligns well with the H I warp observed by Rupen (1991), which makes us believe that we have found evidence for star formation well beyond the disk cutoff. The type of population making up this region will be constrained by future colour studies. Hence we have confirmed the existence of the marginal stellar warp discussed in earlier papers (e.g. Van der Kruit 1979), and also shown that the optical warp structure most likely extends much further than previously believed. The question whether this is a common behavior of warps or a special case has to await further deep photometric studies of samples of edge-on galaxies before it can be answered.

We also confirmed the constancy of scale height with radius, as well as the presence of a photometric thick disk, as revealed in photographic data by Van der Kruit & Searle (1981a) and Jensen & Thuan (1982). Further investigations of more edge-on galaxies are needed to resolve the problem of the thick disk - bulge connection, as proposed by Van der Kruit & Searle (1981a) and further discussed by Morrison et al. (1994), namely whether galaxies with prominent bulges also possess thick disks. Deep colour studies will also be needed to address the question of colour gradients outside $|z| \geq 1'$ (2.9 kpc), which was hinted

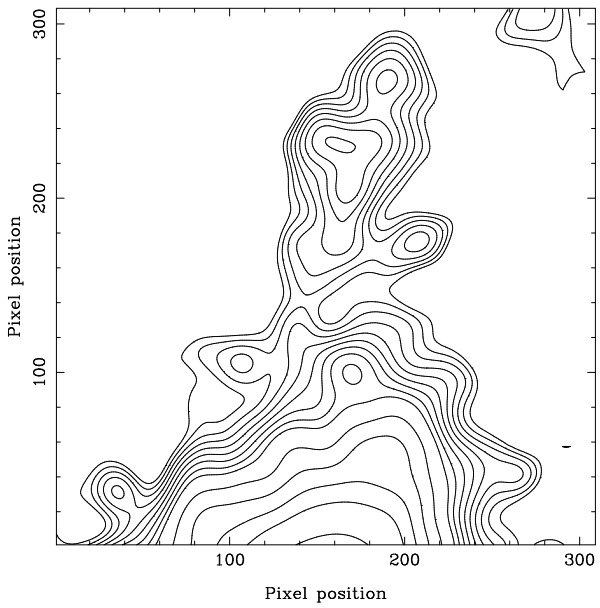

Fig. 9. A contour plot of the NW edge of the disk (lower part) and the extended warp region (upper part). The contours of the extended region are between μ_V = 26.6 mag/□″ and μ_V = 27.3 mag/□″. North is up and east is to the left.

in Jensen & Thuan (1982). The vertical profiles obtained at different radii agree well (with an appropriate shift) down to μ_V = 28 mag/□″ and do *not clearly* display an r^{-2} density profile as the one reported by Sackett et al. (1994) and Lequeux et al. (1996) for NGC 5907. The more complex structure of this galaxy makes it difficult to photometrically separate a possible r^{-2} function and as a result of this we found that several different combinations of functions provide equally good solutions.

Acknowledgements. We would like to thank M. Rupen for letting us use his H I image and the IAC for lending us their CCD. The referee, Dr. B. Fort, is acknowledged for valuable comments and suggestions that improved this presentation. M. N. would like to thank Martin Shaw for comments 'over the net' and Adrick Broeils, Robert Cumming, Stefan Larsson and P O Lindblad for discussions 'in situ'. M. Buontempo, B. Argyle and D. W. Evans at the Carlsberg Telescope are acknowledged for supplying extinction values quickly.

References

Baldwin J. E., Lynden-Bell D., Sancisi R., 1980, MNRAS 193, 313
Barteldrees, A., Dettmar, R. J., 1994, A&AS 103, 475
Block D. L., Bertin G., Stockton A., et al., 1994, A&A 288, 365
Broeils A. H., 1992, Dark and visible matter in spiral galaxies, Ph. D. thesis, University of Groningen
Capaccioli M., Vaucouleurs G. de, 1983, ApJS 52, 465
Carney B., Latham D. W., Laird J. B., 1989, AJ 97, 423
Cox A. L., Sparke L. S., Moorsel G. van, Shaw M., 1996, AJ 111, 1505
Dalcanton J., 1996, ApJ 466, 92
Dokkum P. G. van, Peletier R. F., Grijs R. de, Balcells M., 1994, A&A 286, 415
Edvardsson B., Andersen J., Gustafsson B., Lambert D. L., Nissen P. E., Tomkin J., 1993, A&A 275, 101
Florido E., Prieto M., Battaner E., Mediavilla E., Sanchez-Saavedra M. L., 1991, A&A 242, 301
Fuchs B., 1995, A&A 303, L13
Geus E. de, Vogel S., Digel S., Gruendl R., 1993, ApJ 413, L97
Grijs R. de, Kruit P. C. van der, 1996, A&AS 117, 19
Hamabe M., Kodaira K., Okamura S., Takase B., 1980, PASJ 32, 197
Hegyi D. J., Gerber G. L., 1977, ApJ 218, L7
Jensen E. B., Thuan T. X., 1982, ApJS 50, 421 (JT)
Jörsäter S., 1991, NOT News No. 4, 9
Kormendy J., Bruzual G., 1978, ApJ 223, L63
Kruit P. C. van der, 1979, A&AS 38, 15
Kruit P. C. van der, 1988, A&A 192, 117
Kruit P. C. van der, Searle L., 1981a, A&A 95, 105 (KS81a)
Kruit P. C. van der, Searle L., 1981b, A&A 95, 116
Lequeux J., Allen R. J., Guilloteau S., 1993, A&A 280, L23
Lequeux J., Dantel-Fort M., Fort B., 1995, A&A 296, L13
Lequeux J., Fort B., Dantel-Fort M., Cuillandre J.-C., Mellier Y., 1996, A&A 312, L1
Morrison H. L., Boroson T. A., Harding P., 1994, AJ 108, 1191
Näslund M., 1995, Licentiate thesis, Stockholm University
Näslund M., Jörsäter S., 1995, An Optical Search for Dusty Disks. In: Davies J. I., Burstein D. (eds.) The Opacity of Spiral Disks, NATO Advanced Research Workshop. Kluwer, Dordrecht, p. 189
Pfenniger D., Combes F., Martinet L., 1994, A&A 285, 79
Richter O.-G., Sancisi R., 1994, A&A 290, L9
Rix H.-W., Zaritsky D., 1995, ApJ 447, 82
Robin A. C., Haywood M., Crézé M., Ojha D. K., Bienaymé O., 1996, A&A 305, 125
Rupen M. P., 1991, AJ 102, 48
Sackett P. D., Morrison H. L., Harding P., Boroson T.A., 1994, Nat 370, 441
Sancisi R., 1976, A&A 53, 159
Shaw M. A., 1995, private communication
Shaw M. A., Gilmore G., 1989, MNRAS 237, 903
Shaw M. A., Gilmore G., 1990, MNRAS 242, 59
Valentijn E. A., 1990, Nat 346, 153
Valentijn E. A., 1991, Opaque Spiral Disks: Some Empirical Facts and Consequences. In: Bloemen (ed.) Proc. IAU Symp. 144, The Interstellar Disk-Halo Connection in Galaxies. Kluwer, Dordrecht, p. 245

This article was processed by the author using Springer-Verlag LaTeX A&A style file *L-AA* version 3.